J|A|C|S
ARTICLES
Published on Web 03/03/2006

The Role of Exciton Hopping and Direct Energy Transfer in the Efficient Quenching of Conjugated Polyelectrolytes

Jürgen G. Müller,† Evrim Atas, Chunyan Tan,‡ Kirk S. Schanze,* and Valeria D. Kleiman*

Contribution from the Department of Chemistry, University of Florida, Gainesville, Florida 32611-7200

Received August 29, 2005; E-mail: kleiman@chem.ufl.edu; kschanze@chem.ufl.edu

Abstract: The dynamics of fluorescence quenching of a conjugated polyelectrolyte by a cyanine dye are investigated by femtosecond fluorescence up-conversion and polarization resolved transient absorption. The data are analyzed with a model based on the random walk of the exciton within the polymer chain and a long-range direct energy transfer between polymer and dye. We find that rapid intrachain energy migration toward complex sites with the dye leads to the highly efficient energy transfer, whereas the contribution from direct, long-range energy transfer is negligible. We determine the actual density of complexes with the dye along the polymer chain. A clear deviation from calculations based on a constant complex association constant is found and explained by a reduced effective polymer concentration due to aggregation. Altogether, the quenching efficiency is found to be limited by (i) the energetic disorder within the polymer chain and (ii) the formation of loose polymer aggregates.

1. Introduction

Organic semiconductors and in particular π-conjugated polymers have entered numerous fields of applications such as light-emitting diodes, lasers, solar cells, and recently also the important field of chemical and biological sensing. For biological applications, the π-conjugated polymers need to be soluble in aqueous environments. Recently, fluorescence quenching of a water-soluble π-conjugated polyelectrolyte has been demonstrated with a series of cationic quenchers.[1] π-Conjugated polymers can be quenched very efficiently, a process that cannot be explained by a diffusion-controlled mechanism.[1−3] The efficiency of fluorescence quenching relies on the high mobility of the photoexcitations on the conjugated polymer chain, leading to the quenching of many chromophores upon the binding of a single quencher molecule.[4] However, a variety of effects enhance the fluorescence quenching of conjugated polyelectrolytes (CPEs). In addition to the importance of the photoexcitation mobility along the polymer chain, quencher-induced aggregation of the polymer chain increases the number of chromophores in the direct vicinity of the quencher and enables interchain energy migration, thereby enhancing the quenching efficiency.[1,4] Furthermore, the large charge of the conjugated polyelectrolyte can increase the local quencher concentration by more than an order of magnitude.[5] The influence of these rather extrinsic effects raises the question, to what extent does the exciton mobility on the polymer chain contribute to the fluorescence quenching?

The rate and efficiency of intramolecular energy transfer in π-conjugated polymers is currently a subject of intense discussion. Recent investigations of a PPV-type conjugated polymer found the intrachain energy transfer to be slow and short-range.[6] This is supported by measurements and Monte Carlo modeling of the photoluminescence anisotropy decay of MEH-PPV[7] and polythiophene[8] in dilute solution, giving a range of the energy transfer of only 6−8 conjugated segments, corresponding to about 20−30 nm. On the other hand, enormous conjugated polyelectrolyte luminescence quenching indicates a very efficient intramolecular energy transfer in a water and methanol-soluble PPE.[1,4] Efficient energy transfer on conjugated polymer chains has also been found in single-molecule studies,[9−11] where it was suggested that the energy transfer efficiency depends strongly on the polymer chain conformation, and quenching of the complete chain is achieved only for dense conformations forming aggregated structures. In these studies[10] as well as in investigations in Langmuir−Blodgett films,[12] a three-dimensional exciton

† Current address: Light Technology Institute, University of Karlsruhe, Germany.

‡ Current address: Department of Chemistry, Northwestern University, Evanston IL.

(1) Tan, C. Y.; Atas, E.; Müller, J. G.; Pinto, M. R.; Kleiman, V. D.; Schanze, K. S. *J. Am. Chem. Soc.* **2004**, *126*, 13685−13694.
(2) Zhou, Q.; Swager, T. M. *J. Am. Chem. Soc.* **1995**, *117*, 7017−7018.
(3) Wang, D. L.; Gong, X.; Heeger, P. S.; Rininsland, F.; Bazan, G. C.; Heeger, A. J. *Proc. Natl. Acad. Sci. U.S.A.* **2002**, *99*, 49−53.
(4) Tan, C. Y.; Pinto, M. R.; Schanze, K. S. *Chem. Commun.* **2002**, 446−447.
(5) Wang, J.; Wang, D. L.; Miller, E. K.; Moses, D.; Bazan, G. C.; Heeger, A. J. *Macromolecules* **2000**, *33*, 5153−5158.
(6) Nguyen, T. Q.; Junjun, W.; Doan, V.; Schwartz, B. J.; Tolbert, S. H. *Science* **2000**, *288*, 652−656.
(7) Grage, M. M. L.; Wood, P. W.; Ruseckas, A.; Pullerits, T.; Mitchell, W.; Burn, P. L.; Samuel, I. D. W.; Sundström, V. *J. Chem. Phys.* **2003**, *118*, 7644−7650.
(8) Grage, M. M.-L.; Pullerits, T.; Ruseckas, A.; Theander, M.; Inganas, O.; Sundstrom, V. *Chem. Phys. Lett.* **2001**, *339*, 96−102.
(9) VandenBout, D. A.; Yip, W. T.; Hu, D. H.; Fu, D. K.; Swager, T. M.; Barbara, P. F. *Science* **1997**, *277*, 1074−1077.
(10) Huser, T.; Yan, M.; Rothberg, L. J. *Proc. Natl. Acad. Sci. U.S.A.* **2000**, *97*, 11187−11191.
(11) Müller, J. G.; Lemmer, U.; Raschke, G.; Anni, M.; Scherf, U.; Lupton, J. M.; Feldmann, J. *Phys. Rev. Lett.* **2003**, *91*, 267403.
(12) Levitsky, I. A.; Kim, J. S.; Swager, T. M. *J. Am. Chem. Soc.* **1999**, *121*, 1466−1472.

10.1021/ja055630l CCC: $33.50

Chart 1. Conjugated Polyelectrolyte PPESO3 and Cyanine Dye HMIDC

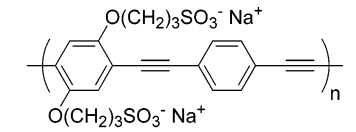

PPESO3

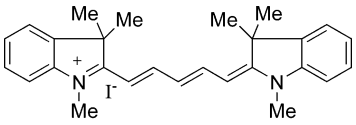

HMIDC

migration was proposed to explain the high quenching efficiency. Altogether, many different mechanisms can improve or limit the quenching efficiency of fluorescence from a conjugated polyelectrolyte. A fundamental understanding of the energy transfer mechanisms in CPEs is therefore crucial for the development of reliable and sensitive polymer-based sensors.

In general, energy transfer between an excited chromophore on a CPE chain and an acceptor molecule can occur (i) by direct energy transfer, (e.g. by a long-range Förster-type dipole−dipole coupling) and (ii) in a multistep mechanism consisting of intrachain energy migration (short-range incoherent hopping) on the polymer chain to a site adjacent to the acceptor, followed by short-range energy transfer to the acceptor. Furthermore, for samples in solution one has to distinguish between quenching by acceptors that are in an ionic complex with the CPE and diffusional quenching by free acceptors in the solution, where the latter becomes important at high quencher concentrations.[5]

Wang et al. described the fluorescence quenching of a PPV-type CPE by methyl viologen with a modified Stern−Volmer equation that accounts for static quenching by both acceptor molecules in an ionic complex with the donor and free acceptors in the solution.[5] The superposition of both contributions leads to an exponential rise of the quenching efficiency according to $I_0/I = (1 + K_{SV}[Q])\cdot\exp(\alpha V)$, were I_0/I is given by the ratio of donor emission without and with the quencher present, K_{SV} represents the association equilibrium constant for complex formation, and V is the volume of the quenching sphere. The factor α accounts for an enhanced quencher concentration in the vicinity of the CPE. The formula is derived on the assumption that the quenching is entirely *static*, i.e., much faster than the excited-state lifetime of the (unquenched) donor. There is ample evidence, however, that exciton migration in conjugated polymers is active on a time scale of tens of picoseconds[8,13] (i.e., comparable to the excited-state lifetime of most polymers). Thus, the quenching should be a *dynamic* process where the rate of energy migration on the CPE chain significantly influences the quenching efficiency.

In this work, we present a detailed study of the energy transfer dynamics from an anionic conjugated poly(phenylene ethynylene) sulfonate (PPESO3) to a cationic dye molecule (HMIDC). The structures are shown in Chart 1. Steady-state fluorescence spectroscopy reveals that formation of an ionic complex between the polymer and dye leads to efficient polymer dye energy transfer.[1] To monitor the energy transfer dynamics, we employ

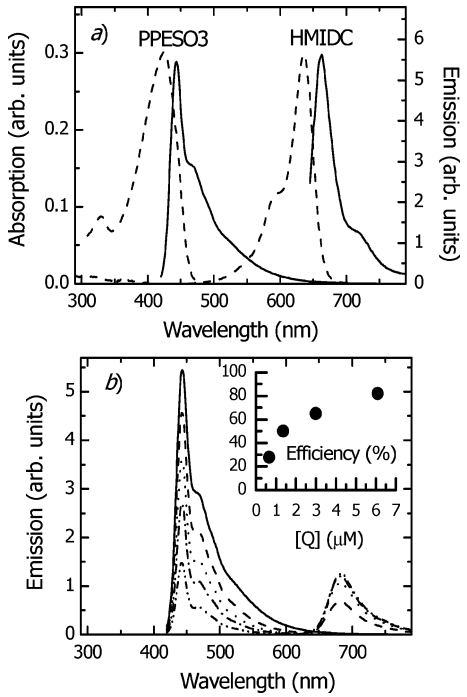

Figure 1. (a) Absorption (− − −) and emission spectra (—) of PPESO3 and HMIDC in methanol. (b) Fluorescence spectra of 10 μM PPESO3 with added HMIDC (0−2.5 μM), $\lambda_{excitation} = 400$ nm. Inset: efficiency of polymer (34 μM) quenching versus dye concentration. At dye concentrations larger than 2 μM, the quenching efficiency saturates.

femtosecond time-resolved fluorescence up-conversion along with transient absorption and polarization anisotropy studies on solutions with systematically varied dye concentration.

A numerical modeling is presented using the analytical solution of a random walk process between energetically identical and equidistant chromophores. The effects induced by energetic and conformational disorder are accounted for by a time-dependent hopping rate. Modeling of the energy transfer dynamics allows us to determine the density of complexes on the polymer chain and the number of chromophores quenched by each complex formed. The individual contributions of intrachain hopping toward the acceptor and direct long-range transfer are quantified, allowing design rules for systems with improved sensor activity to be provided.

2. Experimental Methods and Numerical Calculations

The synthesis of PPESO3 has been described recently.[4] The molecular weight of the polymer is estimated to be $M_n = 100$ kDa, corresponding to about 200 monomer units (see Chart 1 for repeat unit structure). HMIDC was purchased from Aldrich and used as received.

Steady-state absorption and emission spectra of both materials in methanol solution are shown in Figure 1a. The emission of PPESO3 partially overlaps with the HMIDC absorption spectrum, thus enabling singlet energy transfer from the polymer to the dye. The large separation of the emission bands of the polymer and dye allows for independent measurement of donor emission and acceptor emission in time-resolved fluorescence experiments. A concentration of 34 μM PPESO3 in CH_3OH (in polymer repeat units, PRU) was used for the time-resolved fluorescence and transient absorption experiments.

2.1. Time-Resolved Experiments. Excitation pulses are derived from an optical parametric amplifier (OPA) pumped by a commercial Ti:Sa laser system consisting of a Ti:Sa oscillator (Spectra-Physics, Tsunami) and a subsequent Ti:Sa amplifier (Spectra-Physics, Spitfire) with a repetition rate of 1 kHz. The fourth harmonic of the idler is

(13) Herz, L. M.; Silva, C.; Friend, R. H.; Phillips, R. T.; Setayesh, S.; Becker, S.; Marsitsky, D.; Müllen, K. *Phys. Rev. B* **2001**, *64*, 195203.

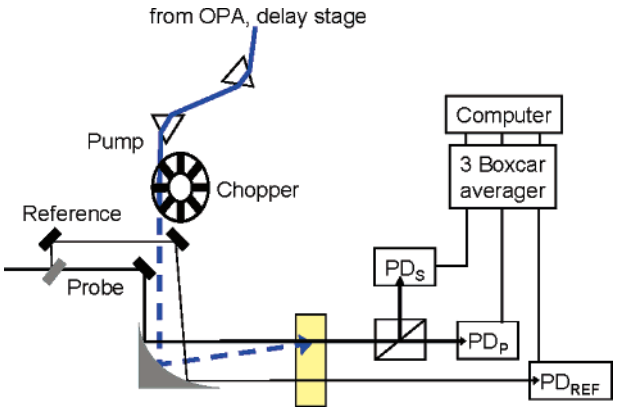

Figure 2. Experimental setup of the transient absorption experiment. After the sample, a Glan−Taylor polarizer splits the probe beam into its polarization components parallel (P) and perpendicular (S) to the pump polarization, respectively. Each of the photodiode signals is integrated separately and shot-by-shot with a Boxcar averager and transferred to a computer.

tuned to the absorption maximum of PPESO3 at 425 nm and fed through a prism compressor, yielding a pulse length of less than 100 fs (fwhm).

In the time-resolved fluorescence experiments,[14,15] a fraction of the Ti:Sa amplifier output is used as the gate pulse (fwhm = 60 fs, 30 μJ/pulse). Fluorescence and gate pulses are overlapped in a nonlinear crystal (β-BBO), and a new beam is generated at the sum frequency. The up-converted light is spectrally filtered using a grating monochromator, detected with a photomultiplier and the signal gated with an integrating boxcar. A variable time delay between excitation and gate pulses allows the ultrafast temporal mapping of the fluorescence.

In the transient absorption experiments[15] sketched in Figure 2, a fraction of the Ti:Sa amplifier output is focused on a 1-mm sapphire plate to generate a white-light continuum, which is used as probe and reference beams. The white light is spectrally filtered, yielding pulses of 10-nm bandwidth centered at 680 nm with a pulse length of ∼100 fs. Using a thin-film polarizer, we oriented the probe light polarization 45° with respect to the pump pulse. After passing through the sample, a Glan-Taylor polarizer splits the probe beam into its polarization components, parallel and perpendicular with respect to the pump, allowing for the simultaneous detection of both polarizations. Pump-induced absorption changes of both probe polarization components are measured as a function of pump−probe time delay by modulation of the pump beam with a mechanical chopper and detection of the probe beams and a reference beam using matched photodiodes and boxcar integration.

The temporal evolution of anisotropy is obtained by evaluation of

$$r(t) = \frac{\Delta A_P(t) - \Delta A_S(t)}{\Delta A_P(t) + 2\Delta A_S(t)} \qquad (1)$$

where $\Delta A_P(t)$ and $\Delta A_S(t)$ correspond to the transient absorption of the polarization oriented parallel or perpendicular to the excitation beam polarization, respectively.

2.2. Numerical Modeling. To obtain information about the complex density on the CPE and the number of monomers quenched by a single acceptor, numerical simulations of the intrachain excitation migration and quenching were performed.

The quenching of mobile excitations on a one-dimensional chain with trap sites has been treated intensively experimentally and in analytical and numerical calculations.[16−22] Monte Carlo simulations of the energy transfer in polythiophene and MEH-PPV found that the energy migration covers on average a region of 6−8 hopping steps around the originally excited conjugated segment, corresponding to a distance of about 30 nm.[7,8] The Förster radius R_0 for energy transfer from PPESO3 to HMIDC is 49 Å.[1] If the initially excited segment on the polymer is closer to the quencher, then direct transfer can play a significant role in the energy transfer. Hence, in our numerical model, the quenching of PPESO3 photoluminescence by the complexed acceptor dye is assumed to occur (i) due to the random walk of excitations on the polymer to the complex site and (ii) by a direct long-range transfer to the complexed acceptor molecules. Energy transfer to free dye molecules in solution can be excluded on the basis of anisotropy measurements as described in the Results section.

Random Walk for Exciton Migration. The conjugated polymer is considered to have excitations localized on conjugated segments of equal length (conjugation length, *cl*; for oligo-*p*-PE, the conjugation length is at least 8−9 monomers or ∼60 Å[23,24]). The excitations migrate on the polymer chain by nearest-neighbor hopping between conjugated segments, until the hopping is terminated by radiative or nonradiative decay of the excitation or by reaching a site that is in an ionic association with an acceptor molecule. In the latter case, instantaneous energy transfer to the acceptor occurs.

Energetic disorder within the polymer chain slows the hopping process with time because segments of comparatively low energy get populated, acting as shallow traps. Monte Carlo methods have been employed to simulate exciton migration on the energy landscape of a disordered polymer chain with varying lengths of conjugated segments.[7,8,13,25,26] This method, however, requires a detailed model of the polymer's geometrical structure and energy landscape.

The numerical modeling presented here (for a detailed mathematical description of the modeling, see Supporting Information) reduces the computational effort significantly. It uses a different approach, solving analytically the random walk process between energetically identical and equidistant chromophores in a numerically solved rate equation model. The energetic and conformational disorder-induced effects are accounted for by a semiempirical time-dependent hopping rate. In essence, the hopping rate slows as the excitation becomes trapped in segments of lower energy.

The slowdown of the hopping rate τ_{hop} is given by the energy barrier ΔE between the currently occupied chromophore and neighboring chromophores, which increases on average with time as the excitation moves to sites of lower energy. Considering a one-dimensional chain with site disorder, the time dependence of the hopping time becomes

(14) Atas, E.; Peng, Z.; Kleiman, V. D. *J. Phys. Chem. B* **2005**, *109*, 13533−13560.

(15) Samples were prepared under degassed conditions. The time-resolved fluorescence experiments were performed under degassed conditions (using a circulating system) and repeated in a fast-rotating sample cell, which ensures that each laser shot (1-ms intervals) illuminates a fresh sample volume. The results were the same, showing that the presence of oxygen during the experiment does not cause changes in the polymer structure or the excitation dynamics. In addition, we checked for photodegradation by comparing sample absorption and emission as measured before and after the experiments.

(16) Rosenstock, H. B. *J. Soc. Ind. Appl. Math.* **1961**, *9*, 169−188.
(17) Montroll, E. W. *J. Math. Phys.* **1969**, *10*, 753.
(18) Fitzgibbon, P. D.; Frank, C. W. *Macromolecules* **1982**, *15*, 733−741.
(19) Klafter, J.; Blumen, A.; Zumofen, G. *J. Stat. Phys.* **1984**, *36*, 561−577.
(20) Palszegi, T.; Sokolov, I. M.; Kauffmann, H. F. *Macromolecules* **1998**, *31*, 2521−2526.
(21) Scheidler, M.; Lemmer, U.; Kersting, R.; Karg, S.; Riess, W.; Cleve, B.; Mahrt, R. F.; Kurz, H.; Bässler, H.; Gobel, E. O.; Thomas, P. *Phys. Rev. B* **1996**, *54*, 5536−5544.
(22) Kauffmann, H. F.; Mollay, B.; Weixelbaumer, W. D.; Burbaumer, J.; Riegler, M.; Meisterhofer, E.; Aussenegg, F. R. *J. Chem. Phys.* **1986**, *85*, 3566−3584.
(23) Kukula, H.; Veit, S.; Godt, A. *Eur. J. Org. Chem.* **1999**, 277−286.
(24) Sluch, M. I.; Godt, A.; Bunz, U. H. F.; Berg, M. A. *J. Am. Chem. Soc.* **2001**, *123*, 6447−6448.
(25) Beljonne, D.; Pourtois, G.; Silva, C.; Hennebicq, E.; Herz, L. M.; Friend, R. H.; Scholes, G. D.; Setayesh, S.; Mullen, K.; Bredas, J. L. *Proc. Natl. Acad. Sci. U.S.A.* **2002**, *99*, 10982−10987.
(26) Meskers, S. C. J.; Hubner, J.; Oestreich, M.; Bassler, H. *J. Phys. Chem. B* **2001**, *105*, 9139−9149.

$$\tau_{hop}(t) = \tau_{hop,0} \cdot \left(\frac{t}{\tau_{hop,0}}\right)^{b/kT} \quad (2)$$

with initial hopping time $\tau_{hop,0} = 1$ ps[25] and energetic disorder parameter b. At very short times, when $t < \tau_{hop,0}$, we assume $\tau_{hop}(t) = \tau_{hop,0}$. The disorder parameter b is used as a fitting parameter.

Direct Förster-Type Energy Transfer. The *direct* Förster-type energy transfer to the complexed acceptor molecules is incorporated in the simulation by assuming that at any time the excitations have an equal probability to reside on any chain segment of length *cl* between two complex sites. The direct transfer rate is calculated by averaging the Förster rate from each of the conjugated segments between two quenchers. Due to the strong distance dependence of $k_{Förster}$, by far the largest contribution to energy transfer by this mechanism is given by the sites adjacent to the complex sites.

Rate Equations for Polymer- and Quencher Populations. The time dependent evolution of the donor- and acceptor excited-state population, $N_{PPESO3}(t)$ and $N_{HMIDC}(t)$, can be obtained by numerical integration of the coupled rate equations

$$\frac{dN_{PPESO3}}{dt} = -N_{PPESO3}(k_{PPESO3} + k_{Förster}) - N_{PPESO3}\frac{p_{quench}(a_{complex},n)}{N_{norm}}k_{hop}$$

$$\frac{dN_{HMIDC}}{dt} = -N_{HMIDC}k_{HMIDC} + N_{PPESO3}k_{Förster} + N_{PPESO3}\frac{p_{quench}(a_{complex},n)}{N_{norm}}k_{hop}$$

$$\frac{dn}{dt} = k_{hop} \quad (3)$$

where k_{PPESO3} and k_{HMIDC} are the excited-state decay rates of PPESO3 in the absence of quenchers and HMIDC, respectively, $k_{hop} = 1/\tau_{hop}$, and p_{quench}/N_{norm} is the probability for an excitation to reach a complex site and be quenched at the random walk step n. To minimize the number of free parameters, and since in the absence of any quencher the excited-state population of the CPE does not decay monoexponentially,[1] we use a stretched exponential function to describe the decay of excited PPESO3 molecules (see Supporting Information).

After numerical integration of eq 3, the measurement signals of the time-dependent photoluminescence yield (PL) and the transient absorption (ΔA) are given by

$$PL(t) = \eta_{PL} \cdot N_{PPESO3}(t)$$

$$\Delta A(t) = -\sigma_{PPESO3} \cdot N_{PPESO3}(t) + \sigma_{HMIDC} \cdot N_{HMIDC}(t) \quad (4)$$

where the prefactor η_{PL} scales the numerical results of the PPESO3 excited-state population to the photoluminescence yield measured in the up-conversion experiment, and σ_{PPE} and σ_{HMIDC} are used to scale the transient absorption signal to the pump-induced population changes of the PPESO3 and HMIDC, respectively.

3. Results

Figure 1b shows the steady-state emission spectra of PPESO3 with different concentrations of added dye. The excitation source at 400 nm exclusively excites the PPESO3 polymer. As the dye concentration is increased, the emission of PPESO3 decreases while the dye emission increases, revealing an efficient energy transfer from the photoexcited polymer to the cyanine dye. This efficient transfer process can be attributed to a complex formation between the anionic polymer donor and the cationic dye acceptor.[1] The inset of Figure 1b shows the efficiency of the PPESO3 fluorescence quenching as a function of dye concentration.

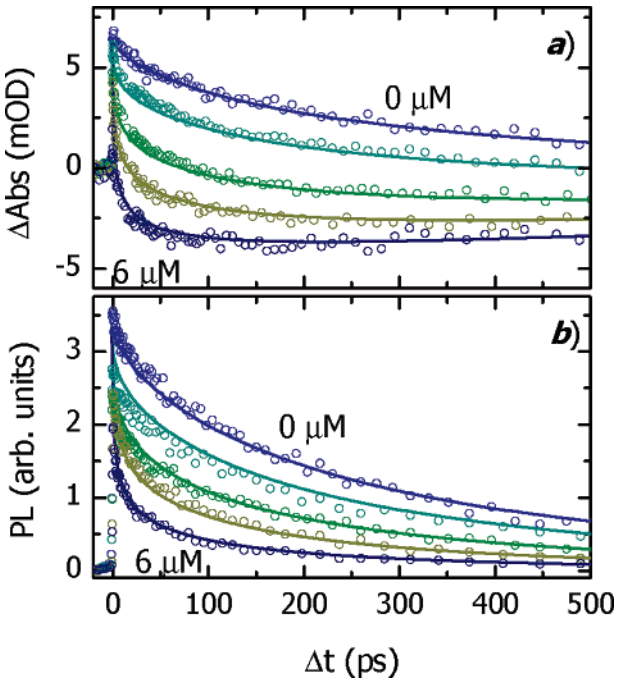

Figure 3. PPESO3 in CH_3OH with added [HMIDC] = 0, 0.65, 1.35, 3, and 6 μM. The excitation wavelength is 425 nm. (a) Transient absorption detected at a probe wavelength of 680 nm. At very early times there is photoinduced absorption from PPESO3. As energy transfer occurs, the PIA decays and stimulated emission from HMIDC grows. (b) Up-conversion signal of PPESO3 fluorescence detected at 450 nm. Both plots present the signal at the magic angle. The results from the numerical calculations are shown as solid lines.

3.1. Transient Absorption and Fluorescence Data. The fluorescence up-conversion experiments allow the study of the energy transfer dynamics from the photoexcited PPESO3 to the cyanine dye. Excitation of the polymer at 425 nm and detection of the fluorescence of PPESO3 at 450 nm yields the temporal response of the polymer's emission (Figure 3b). The topmost curve (0 μM) corresponds to emission from the pure polymer in CH_3OH. The other curves show the emission from the polymer in the presence of different dye concentrations. With increasing dye concentration, the initial amplitude of the fluorescence decreases considerably. This amplitude reduction is assigned to energy transfer from the photoexcited PPESO3 to the dye, occurring on a time scale faster than the experimental time resolution of about 200 fs. Additionally, at high dye concentrations leading to a steady-state quenching of more than 50% (three lower curves), the decay of the PPESO3 fluorescence becomes significantly faster, being reduced from about 250 ps for the pure polymer to 50 ps decay when 6 μM of the cyanine dye is added.

In the following, we will refer to those quenching processes occurring within our instrument time resolution as *static* quenching. The term static does not describe a nonfluorescent ground-state complex in which the polymer π-orbitals are significantly altered by the association with the quencher. Since the absorption spectrum of the PPESO3 does not change with addition of HMIDC, the formation of such complexes is unlikely. Instead, static quenching refers to a very fast energy transfer from the polymer to the quencher, due to an initial excitation of a conjugated segment that is in the direct vicinity of the quencher.

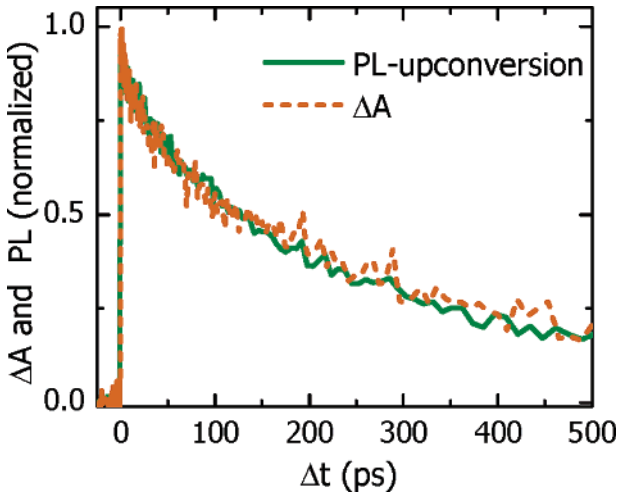

Figure 4. PL up-conversion and Δ*A* of PPESO3. The signals have identical decay dynamics, showing that (i) both signals give the population of the first excited state of PPESO3 and (ii) no significant energy transfer to aggregate sites with a lower radiative decay rate occurs.

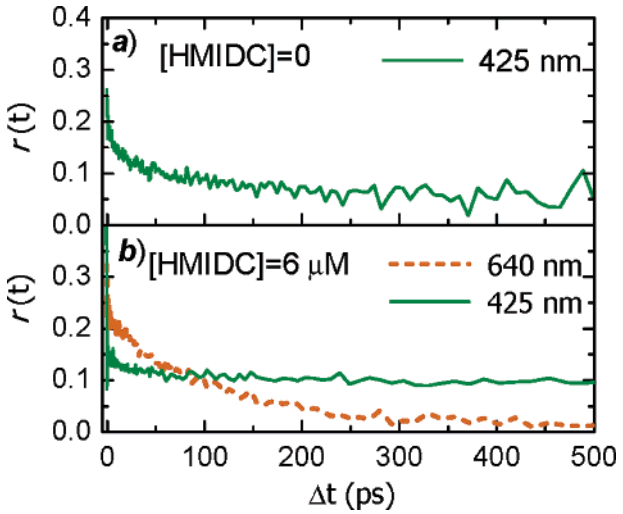

Figure 5. Time-dependent anisotropy detected at 680 nm for (a) PPESO3 in CH_3OH. Excitation at 425 nm. The residual anisotropy at long Δ*t* indicates intrachain energy transfer activity during the entire emission lifetime of the polymer. (b) PPESO3 with 6 μM of HMIDC. Direct excitation of HMIDC at 640 nm shows no residual anisotropy. Excitation at 425 nm shows a residual anisotropy from the HMIDC indicating that the signal arises from molecules in complex with the PPESO3, which maintain their orientation during the time scales of interest.

Quenching taking place on the time scale of the excited-state lifetime will be referred to as *dynamic*. We will later show that the dynamic process is not a quencher diffusional process, but exciton migration within the polymer chain.

Contributions from both static and dynamic quenching are also found in the transient absorption data, which allow monitoring of the excited-state population of PPESO3 and HMIDC simultaneously. The transient absorption of PPESO3 in methanol for different concentrations of cyanine dye is shown in Figure 3a. Again the topmost curve corresponds to pure polymer, while the other curves correspond to the transient absorption signal in the presence of the quencher.

Probing at $\lambda = 680$ nm (maximum emission of the dye), the pure polymer solution shows a positive transient absorption (an increase in the absorption of the sample). Figure 4 compares the time evolution of this photoinduced absorption (PIA) signal with the PPESO3 fluorescence decay. The similarity of these two curves allows us to attribute the transient absorption signal at 680 nm to absorption by the singlet exciton of PPESO3. In agreement with the fluorescence up-conversion data, the addition of HMIDC leads to a reduction of the PIA amplitude and decay time. Furthermore, in the presence of the dye the transient absorption data show a crossover from PIA to a negative signal (increased transmission), indicating either ground-state bleaching or stimulated emission. At this probe wavelength, neither PPESO3 nor HMIDC absorb, and the polymer does not fluoresce; therefore, the negative transient absorption is assigned to stimulated emission (SE) from excited HMIDC. Since direct excitation of dye molecules by the pump pulse at λ pump = 425 nm does not occur, the increase of SE with delay time reflects the energy transfer to the dye. Excitation energy leaving the polymer reduces the PIA from the PPESO3 (decrease of Δ*A*), while energy arriving on the dye enhances SE, again decreasing the measured signal Δ*A*. The combination of both effects induces a strong change in the transient absorption signal and results in a high sensitivity to the energy transfer dynamics.

3.2. Anisotropy and Ionic Complexes. Figure 5a shows the anisotropy evaluated from the transient absorption data using eq 1. The pure polymer sample features an anisotropy of $r_0 = 0.3$ at $\Delta t = 0$, which is slightly lower than the theoretical value of $r_0 = 0.4$ expected for a three-dimensional, randomly oriented ensemble of perfectly linear transition dipoles.[27] The reason for this lower starting value is an ultrafast process occurring within the experimental time resolution of ca. 150 fs. One possible explanation for this fast loss of anisotropy is the dynamic localization of the excitations due to torsional motions on the polymeric chain. For MEH-PPV, loss of anisotropy has been shown to occur in <100 fs.[28] After this initial decay, any subsequent loss of anisotropy is a direct measure of the exciton hopping between conjugated segments of different orientation.[8,29] The large molecular weight of the polymer chain slows the rotational diffusion, leading to an almost static orientation of the molecule on the subnanosecond time scales probed here.

The anisotropy decays within about 150 ps. A complete randomization of dipole orientations is expected to lead to $r_\infty = 0$, which is in contrast to the residual anisotropy of $r_\infty = 0.05$ observed in the data. On the basis of the long-lived anisotropy decay, we conclude that intrachain energy transfer on the polymer is active during the entire lifetime (250 ps) of the photoexcitations. The crossover from a fast initial decay to an extremely slow decay at larger time delays, however, indicates a significant slowdown of the hopping process with time due to energetic disorder within the CPEs, leading to weak trapping of the excitations.[30]

Transient absorption anisotropy changes in the presence of HMIDC were examined to understand the role of HMIDC molecules associated with the polymer versus free dye molecules on the energy transfer. In the presence of 6 μM of HMIDC (corresponding to ~80% quenching of the steady-state polymer emission), the anisotropy dynamics show a drastic change. Figure 5b shows the anisotropy detected after excitation with

(27) Valeur, B. *Molecular Fluorescence: Principles and Applications*, 1st ed.; Wiley-VCH: Weinheim, 2002; p 147.
(28) Ruseckas, A.; Wood, P.; Samuel, I. D. W.; Webster, G. R.; Mitchell, W. J.; Burn, P. L.; Sundström, V. *Phys. Rev. B* **2005**, *72*, 115214.
(29) Gaab, K. M.; Bardeen, C. J. *J. Phys. Chem. B* **2004**, *108*, 4619−4626.
(30) Scheidler, M.; Cleve, B.; Bässler, H.; Thomas, P. *Chem. Phys. Lett.* **1994**, *225*, 431−436.

two different pump frequencies, leading to either direct or sensitized dye emission. While probing at 680 nm, which corresponds to the emission peak of the HMIDC, we first excite the sample at 640 nm leading to direct excitation of the HMIDC (at this wavelength, there is no absorption by PPESO3). Consequently, under these conditions the transient absorption signal is given exclusively by stimulated emission of the dye, and the anisotropy calculated thereof is the anisotropy of the HMIDC emission. The corresponding transient anisotropy plot in Figure 5b shows an initial anisotropy of $r_o = 0.35$, close to the theoretical expectation. The decay of the value of the anisotropy to $r_\infty \approx 0$ shows a time constant of about 100 ps.

While still probing the dye emission ($\lambda = 680$ nm), it is possible to investigate the anisotropy behavior after energy transfer by exciting the dye exclusively via energy transfer from the PPESO3. This is accomplished by tuning the excitation wavelength to 425 nm, where the PPESO3 absorption is high and the HMIDC absorption is negligible. Under these conditions, the time-dependent anisotropy shows a weak initial decay. At $\Delta t > 50$ ps, the anisotropy of the sensitized dye emission remains about constant at a level of $r_\infty = 0.1$.

4. Discussion

To understand the quenching mechanisms, it is fundamental to answer the question: do free dye molecules in solution contribute to the quenching? We will first answer this question and then describe the PL up-conversion and transient absorption data quantitatively by comparing it to the results of the numerical simulation. An important outcome of the numerical simulations is that they provide the density of complexes along the polymer chain for the samples with different HMIDC concentrations. As we will discuss below, the computed complex density deviates significantly from expectations based on a constant complex association constant.

4.1. Loss of Anisotropy and the Absence of Quenching by Free Dye Molecules. Figure 5b shows the anisotropy decay of the transient absorption signal measured on the PPESO3/HMIDC mixture. Due to the fast energy transfer to the dye, the transient absorption signal at $\Delta t > 50$ ps is dominated by stimulated emission from dye molecules; the observed anisotropy therefore corresponds to the emission anisotropy of the HMIDC. Direct excitation of the dye leads to a high initial anisotropy of the dye emission of $r_o = 0.35$, decaying to $r_\infty \approx 0$ with a time constant of about 100 ps. Any dye molecules associated with the PPESO3 chain are expected to maintain their orientation during the time scales of interest here. Consequently, we attribute the anisotropy decay down to $r \approx 0$ to the rotation of *free* dye molecules in solution.[31] Figure 3a shows that for the solution with highest dye concentration (6 μM) the energy transfer occurs very rapidly, and at $\Delta t > 50$ ps the transfer from PPESO3 to the dye is almost complete. After completion of the energy transfer, the anisotropy of the sensitized dye emission shown in Figure 5b remains almost constant at $r_\infty = 0.1$. We conclude that the energy is exclusively transferred to dye molecules that are bound to the PPESO3 in an ionic association and cannot freely rotate, which justifies the neglect of quenching by free dye in solution. Note that this result is in contrast to previous studies on the quenching mechanism of a water-soluble poly(phenylenevinylene).[5]

The relatively high value of the residual anisotropy ($r_\infty = 0.1$) obtained for sensitized dye molecules suggests that in the donor−acceptor complex the transition dipole moments of HMIDC molecules are aligned approximately parallel to the PPESO3 backbone. This is in agreement with the slight red shift reported earlier[1] in the emission from the dye when PPESO3 is added to the solution. The constant anisotropy of the sensitized emission from the complexed dye also confirms our previous assumption that rotational diffusion of the polymer chain is much slower than the excited-state lifetime and does not contribute to the anisotropy decay of photoexcitations on the polymer chain. It further implies that the sample volume in solution probed by the polyelectrolyte is much smaller than its radius of gyration, which is in contrast to previous reports.[5]

4.2. Comparison of TA- and PL Up-Conversion Dynamics. The excitation hopping dynamics and hence the anisotropy decay can be strongly affected by the presence of energetic traps formed by interchain interactions in aggregates.[32] In our previous work,[1] we showed that in H_2O (a poor solvent) the polymer tends to aggregate, whereas in CH_3OH (a good solvent) it is present in unaggregated form. Barbara and co-workers described possible conformations of flexible and stiff polymers with and without defects.[33] According to their work, rigid polymers with defects but no intersegment attraction lead to extended conformations with approximately straight-chain segments between defects. Figure 1b shows no sign of aggregation or chain-collapsing conformation. We conclude then that intersegment attractions are not present, and therefore the interchain process will not contribute to the overall excitation migration. Instead, exciton hopping is expected to occur within a given chain. This finding is corroborated by the comparison of the fluorescence up-conversion and transient absorption dynamics shown in Figure 4 from which we concluded that excitation trapping in aggregates does not occur.

Conjugated polymers can form aggregates with radiative decay rates that differ from those of their unaggregated structures.[34] If aggregates are formed under the experimental conditions used in the present investigation, the energy transfer to the aggregates would be expected to change the radiative decay rate. The photoluminescence up-conversion signal is given by $PL_{up} \approx N(S_1) \cdot k_{rad}$, where $N(S_1)$is the population number of excitations of PPESO3 and k_{rad} is the radiative decay rate. Assuming a time-independent cross section for the $S_1 \rightarrow S_{n>1}$ transition, the photoinduced absorption measured in transient absorption is simply given by $\Delta A \approx N(S_1)$. Thus, by comparing fluorescence up-conversion and transient absorption dynamics, it is possible to determine if the radiative decay rate of the polymer changes with time. Since both PL_{UP} and ΔA show exactly the same dynamics (Figure 4), the radiative decay rate is constant in time. We conclude that energy transfer to PPESO3 aggregates does not occur.

4.3. Quenching Dynamics and the Static Contribution. The fluorescence up-conversion data shown in Figure 3b can be used

(31) Direct excitation of the dye probes both free dye molecules in solution and those in the complex. Anisotropy decay to $r \approx 0$ indicates that most dye molecules are free in solution. The contribution to the anisotropy from complexed dye molecules is just too small to be detected.

(32) Grage, M. M. L.; Zaushitsyn, Y.; Yartsev, A.; Chachisvilis, M.; Sundström, V.; Pullerits, T. *Phys. Rev. B* **2003**, *67*, 205207.
(33) Hu, D. H.; Yu, J.; Wong, K.; Bagchi, B.; Rossky, P. J.; Barbara, P. F. *Nature* **2000**, *405*, 1030−1033.
(34) Kamalov, V. F.; Struganova, I. A.; Yoshihara, K. *J. Phys. Chem.* **1996**, *100*, 8640−8644.

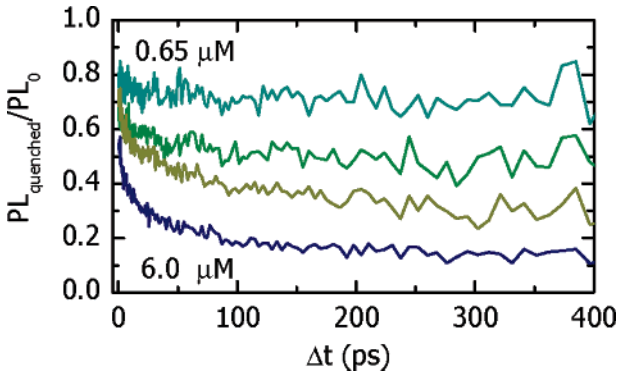

Figure 6. PL of samples containing HMIDC, divided by the PL of pure PPESO3 solution (from Figure 3b). These ratios represent the amount of quenching at a given delay time. At $\Delta t = 0$, the plots represent static component. As the concentration of quencher increases, the contribution from the dynamic component becomes more significant. This contribution is more prominent on solutions with high dye concentration.

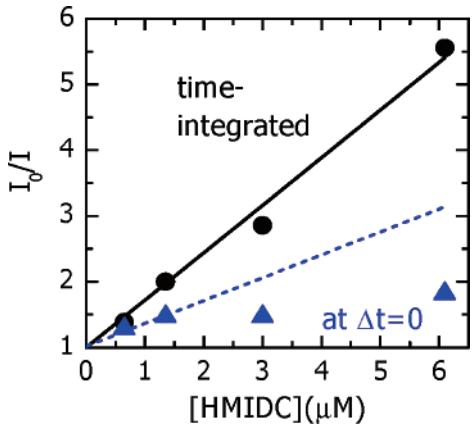

Figure 7. Stern−Volmer plot of the time-integrated photoluminescence (●) and the instantaneous photoluminescence ($\Delta t = 0$, ▲) from the up-conversion experiment. The instantaneous photoluminescence shows a strong saturation at quencher concentrations above 1.2 μM. Even in the absence of saturation, the overall quenching is larger than the static component, indicating the presence of a dynamic contribution.

to estimate the relative contributions of static and dynamic quenching. The temporal evolution of PPESO3 fluorescence in the presence of HMIDC normalized to the fluorescence of the pure CPE sample is shown in Figure 6. This emission ratio represents the amount of quenching at a given delay time. A ratio of 1 indicates that no quenching has occurred up to the given delay time. The lowest quencher concentration of 0.65 μM corresponds to 25% of the steady-state (integrated) polymer emission being quenched by the dye acceptor. For this sample, at $\Delta t \approx 0$ we observe a fluorescence ratio of 0.8, indicating that 20% of the emission is quenched within the experimental time resolution, therefore being regarded as static quenching. At increased delay time the fluorescence ratio appears nearly unchanged, indicating the lack of additional dynamic quenching. At increased quencher concentrations the fluorescence ratio begins to decay with time, revealing additional dynamic quenching. At the highest quencher concentration of 6 μM, about half of the energy transfer is completed within the experimental time resolution (static component), whereas the other half of the energy transfer occurs on a 50-ps time scale (dynamic component). At increased quencher concentrations, the simultaneous presence of static and dynamic quenching is expected to lead to a superlinear Stern−Volmer behavior.[35] Figure 7 shows the fluorescence signal taken from Figure 3b, integrated over time, and plotted versus dye concentration. This figure reveals a linear dependence of I_0/I as a function of dye concentration.[36] Considering a purely static quenching in a 34 μM solution of the polymer, a fit to the Stern−Volmer equation gives an association constant of $\sim 7.2 \times 10^5$ M^{-1}. The time-resolved data allow us to draw an equivalent Stern−Volmer plot for the static component only. It is obtained by plotting the ratio of the PPESO3 fluorescence in the presence and the absence of dye at $\Delta t = 0$, also shown in Figure 7. Above a quencher concentration of ~ 2 μM, the quenching does not increase any further with increased HMIDC concentration. In the time-integrated Stern−Volmer plot, the saturation of the static quenching component "cancels out" the superlinear response expected from simultaneous static and dynamic quenching and leads to an apparent linear increase of the steady-state (time-integrated) quenching with quencher concentration.

(35) Lakowicz, J. R. *Principles of Fluorescence Spectrosocopy*, 2nd ed.; Kluwer Academic/Plenum Publishers: New York, 1999; p 243.
(36) In our previous report, the SV (ref 1) plots for quenching of PPESO3 by HMIDC were slightly superlinear. The difference observed here is because the ultrafast experiments were performed at higher polymer concentrations.

Table 1. Parameters and Variables Used in the Numerical Simulations and Fitting of the Time-Resolved PL Up-Conversion and the Transient Absorption Data[a]

fixed parameters		variables	
$1/k_{PPESO3}$[b]	250 ps	b/kT	0.8
$1/k_{HMIDC}$[c]	1700 ps	η_{PL}	0.33
β[b]	0.6	σ_{PPESO3}	1.47
$\tau_{hop,0}$[d]	1 ps	σ_{HMIDC}	1.25
cl[e]	6.1 nm		

[a] All parameters are identical for the different samples. [b] Obtained from the PL up-conversion of pure PPESO3 in CH_3OH. [c] Taken from ref 1. [d] Taken from ref 25. [e] Taken from ref 23.

4.4. Quenching and the Role of the Dynamic Component. The quenching dynamics are affected both by the average distance between quencher complexes along the PPESO3 chain and by the excitation hopping dynamics. The numerical simulations discussed in this section pinpoint the reasons for the saturation of static quenching at high quencher concentrations and the unexpected linear Stern−Volmer plot obtained from steady-state measurements. The time-resolved PL up-conversion and transient absorption data are simulated using eq 4. The free variables are the *disorder parameter b*, determining the excitation hopping dynamics; the average *complex distance* $a_{complex}$; the *scaling factors* η_{PL} for the fitting of the photoluminescence up-conversion data; and σ_{PPESO3} and σ_{HMIDC} for the fitting of the transient absorption data. Using a single set of parameters it is possible to fit the five independent PL up-conversion and transient absorption datasets.

The overall fits to all the samples with a unique set of parameters are shown as solid lines in Figure 3. Good agreement between the simulations and the experimental data was achieved for both the up-conversion and transient absorption at all quencher concentrations. Table 1 summarizes the parameters used for all samples.

The distance between complexes formed along the polymer chain ($a_{complex}$) obtained from the numeric modeling of the time-resolved quenching dynamics allows one to determine how many polymer repeat units are actually quenched by a single PPESO3/dye complex. The lowest dye concentration of $[Q_0]$

Table 2. Average Distance between Two Acceptor Molecules in Complex with the PPESO3[a]

[Q] (μM)	$a_{complex}$ (in segments)	$a_{complex}$ (in PRU) 1 segment = 4.5 PRU[b]
0.65	23	104
1.5	11	49
3	8	36
6	6	27

[a] These values are used to generate the curves shown in Figure 3. [b] Taken from ref 23.

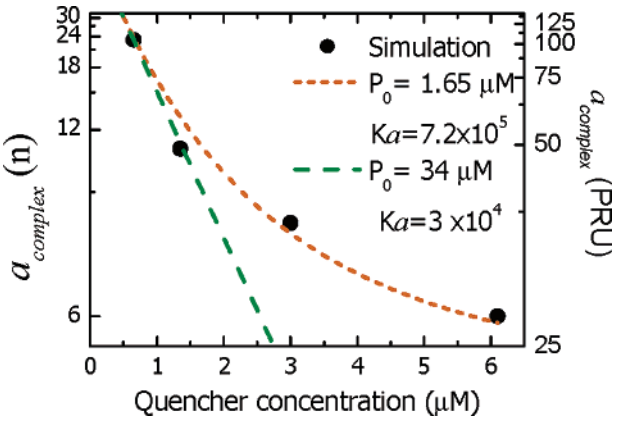

Figure 8. Average distance between quencher molecules complexed with the PPESO3 on a reciprocal scale. Results from the numerical model are shown, a fit within the linear regime (– – –) yields a relatively lower association constant. A good match between eq 5 and the model is achieved by using a reduced conjugated polymer concentration of $[P_0] = 1.65$ μM, indicating an effective reduction in the number of polymer sites available to form complexes.

$= 0.65$ μM leads to an integrated quenching of 25% of the polymer repeat units by forming one complex per 104 PRU (see Table 2). This corresponds to about 26 PRU (35.4 nm) quenched by a single dye molecule.

Figure 8 shows the most important result of the simulations: the average distance between complexes on the PPESO3 chain. The left axis shows the complex distance in hopping steps ($a_{complex}$, in units of *cl*), which is the natural unit used in the random walk simulations. By assuming a length of the conjugated segments (*cl*) of about 8−9 phenylene ethynylenes,[23,24] which corresponds to 4.5 PRU, the complex distance can be expressed in units of PRU (right axis in Figure 8). The results of the numerical simulation range from about 23 segments (104 PRU) in the case of the sample showing the smallest overall quenching (dye concentration $[Q] = 0.65$ μM down to six segments (27 PRU) for the sample with the highest quenching concentration ($[Q] = 6$ μM).

If we assume purely static quenching and a 1:1 PPESO3/HMIDC complex,[1] the distance between complex sites can also be evaluated analytically. Using the association equilibrium constant K_a and the initial CPE and dye concentrations, we obtain the concentration of complexes in solution

$$[PQ] = \left[\frac{[P_0] + [Q_0] + K_a^{-1}}{2} - \sqrt{\left(\frac{[P_0] + [Q_0] + K_a^{-1}}{2}\right)^2 - [P_0][Q_0]}\right] \quad (5)$$

where $[P]$ and $[Q]$ are the corresponding concentrations of uncomplexed molecules and $[PQ]$ is the concentration of PPESO3/HMIDC complexes. This equation is derived assuming that all PRU are accessible to form PPESO3/HMIDC complexes. As shown below, this is apparently not the case for solutions with high dye concentration.

The ratio of the initial polymer concentration with the concentration of complexes, $\{[P_0]\}/\{[PQ]\}$, gives the average distance between the PPESO3/HMIDC complexes along the polymer chain in PRU and is directly comparable to the complex distance $a_{complex}$ obtained from the numerical model. Figure 8 compares the numerical simulation results and the ratio $\{[PQ]\}/\{[P_0]\}$ obtained from the analytical expression for the association equilibrium. At dye concentrations below 1.2 μM, the equilibrium equation from an assumed 1:1 PPESO3/HMIDC complex ratio leads to an approximately linear decrease of the inverse complex distance with increasing dye concentration.

Using a total polymer concentration of 34 μM, eq 5 behaves linearly for $K_a \approx 3 \times 10^4$ M^{-1}. This association constant is considerably smaller than the one obtained from the Stern−Volmer plot (Figure 7). At dye concentrations above 1.2 μM the numerical results deviate significantly from the linear behavior predicted by a 1:1 PPESO3/HMIDC complex. The reason for this early saturation of complex formation is uncertain. It is clear from Figure 8 that at high HMIDC concentrations the number of complexes formed is smaller than predicted by eq 5. One possibility is that, at these high concentrations, more than one HMIDC molecule interacts with a given complex site. This would effectively increase the distance between complex sites. Attempts to fit the complex distance by considering complexes with different PPESO3/HMIDC ratios were unsuccessful though the simultaneous presence of complexes with one, two, or more HMIDC molecules cannot be completely ruled out.

The onset of the saturation corresponds to an average complex distance of ~30 PRU. Given this large distance, it seems unreasonable to attribute the effect to mutual electrostatic repulsion between complex sites. It is more likely that the effect arises due to formation of a loose aggregate of the PPESO3 chain, which effectively reduces the polymer surface area available to the dye in solution. Loose aggregates are defined as aggregates that contain both the polyelectrolyte and the counterions, as opposed to dense aggregates where different branches of the polymer are in van der Waals contact.[37] Within these loose polyelectrolyte aggregates, the electrostatic interactions between the quencher molecules might be changed. Note that the PPESO3 photoluminescence spectra clearly exclude significant electronic interchain interactions such as $\pi-\pi$ stacking of PPESO3 in dilute CH_3OH solutions.[1]

A polymer surface reduced due to the formation of loose aggregates corresponds to an effective reduction of the polymer concentration available for complex formation with the dye. If we consider that the available concentration of PPESO3 to form complexes is smaller than the initial concentration $[P_0]$, we find a good agreement between eq 5 and the numeric modeling using an association constant value of $K_a \approx 7.2 \times 10^5$ M^{-1} and a polymer concentration of $[P_0] \approx 1.65$ μM. Apparently, the tendency of the polymer chain to form loose aggregates lowers the quenching efficiency. In our previous studies[1] on the quenching of PPESO3 by cationic quenchers, we found that

(37) Nomula, S.; Cooper, S. L. *J. Phys. Chem. B* **2000**, *104*, 6963−6972.

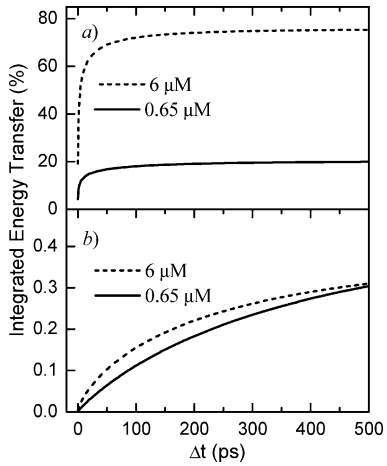

Figure 9. Individual contributions to the integrated energy transfer, (a) random walk mediated and (b) direct-transfer versus time after excitation. For both samples, the random walk process dominates the energy transfer. It can be distinguished by the extremely fast decay of its transfer efficiency, leading to about 50% of the total quenching being completed within less than 1 ps.

quencher-induced aggregation of the conjugated polyelectrolytes increases the quenching efficiency significantly. In that case, it is the facilitation of the exciton dynamics through additional interchain hopping of the photoexcitations that enhances the quenching.

The modeling of the quenching dynamics allows the evaluation of the individual contributions to the energy transfer given by (i) the random walk of the excitation to the complex site and (ii) direct (long-range) energy transfer to the complex site. Figure 9 shows the time evolution of the integrated quenching for each mechanism for the samples quenched by 0.65 and 6 μM HMIDC, respectively. For both samples, the random walk gives by far the largest contribution to the total energy transfer. In fact, the random walk seems to be almost the exclusive pathway. The two contributions have distinctly different dynamics: the direct part of the energy transfer rate is time-independent; it depends solely on the Förster radius and the complex concentration. In contrast, the random walk mechanism is intrinsically time-dependent: the probability of an exciton to hop to a new, distinct segment (i.e., the probability of finding the quencher) decreases with time. This behavior is seen in Figure 9 as a steady increase in the direct contribution while an initial contribution followed by flat time dependence is observed for the exciton hopping mechanism. The time dependence found in the random walk is a consequence of the quickly decreasing probability of an excitation to hop to a new, thus-far unvisited site. Even in the limit of a large separation of quencher sites, the probability to find a complex site decays by 75% within only 10 hopping steps. Moreover, the decrease of the average excitation energy due to site disorder leads to a slowdown of the hopping rate by a factor of 5 within 10 ps. This extremely fast decay of the random walk driven energy transfer leads to a large fraction of the energy being transferred on a time scale much faster than the intrinsic excited-state lifetime of the donor. Accordingly, the fast excitation hopping is responsible for the dominating static quenching mechanism found in this material system. For example, for the high quencher concentration sample, at $\Delta t = 5$ ps a 52% (integrated) quenching has already occurred through the random walk of the excitations, while for the low quencher concentration sample the quenching by random walk has already reached 12%. For both samples, the contribution from the direct mechanism is negligible on this time scale.

The reason for the small contribution from the long-range mechanism is the size of the conjugated segments (*cl*). Due to the r^6 dependence of the Förster mechanism, using a smaller *cl* parameter leads to a larger contribution to the overall quenching. For a *cl* corresponding to 4.5 PRU (8−9 rings) the numerical simulations show that, at low quencher concentrations, the direct contribution accounts for only 1.5% of the total energy transferred to the quencher. Comparison of absorption and emission spectra maxima in this work (425 and 450 nm, respectively) with those obtained from oligomers by Kukula et al.[23] and by Sluch et al.[24] suggests that the use of 8−9 rings as the conjugation length (4.5 PRU) describes a lower limit in the number of monomer units in a conjugation length. If, as we suspect, the conjugation length is even longer, the direct contribution will be even less important.

Though the direct component contribution to the overall quenching is <2%, its time-independent characteristic implies that at long time scales this mechanism is the major contributor to the quenching. However, on long time scales direct quenching must compete with the natural decay of the excitation, and consequenctly, this transfer mechanism remains ineffective and still does not contribute significantly. In conclusion, the dominant mechanism responsible for the fast and effective quenching is the random walk of the excitations within the polymer chain.

As shown above, the amplification of fluorescence quenching in the PPESO3/HMIDC arises mainly from the rapid intrachain migration of excitons on the conjugated polyelectrolyte. A reduction of the site disorder would lead to a significant reduction of excitation trapping and thereby further enhance the fluorescence quenching efficiency. In our numerical model, a vanishing disorder leads to a constant hopping rate. In that limiting case, the lowest dye concentration of $[Q_0] = 0.65$ μM would yield a fluorescence quenching efficiency of 97% instead of the 25% found experimentally. The quencher complex concentration needed for 50% quenching would decrease by a factor of 5, corresponding to a dye concentration of only $[Q_0] = 0.25$ μM.

5. Conclusions

The fluorescence quenching dynamics in a solution-based system have been investigated using the conjugated polyelectrolyte PPESO3 as energy donor and the dye HMIDC as acceptor. Numerical modeling of picosecond time-resolved fluorescence up-conversion and transient absorption measurements was carried out on a number of samples with systematically varied quencher concentration. In general, the dynamics show that hopping of the photoexcitations to the complex sites is the dominating pathway for fluorescence quenching. Direct, long-range transfer to the acceptor contributes only about 1.5% to the total energy transfer at low quencher concentrations, and it becomes negligible at elevated quencher concentrations.

Anisotropy measurements lead to the conclusion that all of the quenching occurs with dye molecules bound to the polymer through ionic association. Simulations of the intrachain excitation migration allowed us to calculate the actual density of complexes formed between the ionic donor and acceptor

molecules. We found that at low quencher concentrations (below $[Q_0] = 1.2\ \mu$M) the polyelectrolyte/dye complex density scales approximately linearly with dye concentration, in accordance with the equilibrium equation for a 1:1 complex formation. At higher dye concentrations, however, a saturation of the complex density sets in. From the equilibrium equation, this behavior would be expected at much higher concentrations, when the dye concentration becomes comparable to the monomer concentration of the polyelectrolyte. We suggest that the formation of loose aggregates of the polyelectrolyte leads to a strong decrease of the number of polymer sites that are available to form a complex with the dye. Since no spectroscopic signature of polyelectrolyte aggregate formation has been found, here the term "loose" corresponds to aggregates with an interchain distance being too large to enable electronic interchain interactions (e.g., $\pi-\pi$ stacking), but small enough to hinder complex formation. Satisfactory agreement of the complex densities predicted by the equilibrium equation and those calculated from the numerical simulations of time-resolved data is achieved, if the PPESO3 concentration used in the equilibrium equation is reduced by a factor of 20. The decrease of quenching efficiency induced by the formation of loose aggregates is in contrast to the increase of quenching efficiency usually found in the case of the formation of dense aggregates in strongly polar solvents, where interchain migration of excitations is enabled.

The results also show that the factor limiting the fluorescence quenching efficiency is trapping of the photoexcitations on the PPESO3 conjugated polyelectrolyte. The simulations suggest that a decrease of site disorder within the conjugated polymer chain well below k_BT should lead to an increase of quenching efficiency by a factor of 5.

Acknowledgment. We gratefully acknowledge financial support by the Department of Energy through Grant No. DE-FG02-03ER15484. E.A. acknowledges partial support from the Research Corporation (RI0558).

Supporting Information Available: A detailed description of the numerical calculations. This material is available free of charge via the Internet at http://pubs.acs.org.

JA055630L